Inactivation and recovery in Kv1.4 K^+ channels: lipophilic interactions at the intracellular mouth of the pore

Glenna C. L. Bett and Randall L. Rasmusson

Department of Physiology and Biophysics, School of Medicine and Biomedical Sciences, 124 Sherman Hall, University at Buffalo, The State University of New York, Buffalo, NY 14214-3005, USA

C-type inactivation is present in many voltage-gated potassium channels and is probably related to 'slow' inactivation in calcium and sodium channels. The mechanisms underlying C-type inactivation are unclear, but it is sensitive to mutations on both the extra- and intracellular sides of the channel. We used an N-terminal deleted channel with a valine to alanine point mutation at the intracellular side of S6 (fKv1.4[V561A]ΔN). This construct alters recovery from inactivation and inverts the relationship between C-type inactivation and $[K^+]_o$. We used this inverted relationship to examine C-type inactivation and coupling mechanisms between N- and C-type inactivation. The valine to alanine mutation reduces the channel's affinity for both quinidine and the N-terminal domain. However, binding of the N-terminal or quinidine restores normal recovery from inactivation. This suggests that coupling between N- and C-type inactivation is dominated by allosteric mechanisms. The permeation mechanism, driven by a reduction in permeant $[K^+]_o$ following pore block (which would retard C-type inactivation), contributes minimally to coupling in these channels. We propose that the cytoplasmic half of S6 forms part of the N-terminal binding site, as previously predicted from X-ray crystallography studies in the distantly related KcsA channel. Binding of the N-terminal domain or a positively charged lipophilic compound such as quinidine interacts with the hydrophobic moieties on S6 in the bound state. This binding can orientate S6 into a conformation which resembles the normal C-type inactivated state. This is the probable mechanism by which drug or N-terminal binding increases the rate of C-type inactivation via an allosteric mechanism.

(Received 14 September 2003; accepted after revision 24 October 2003; first published online 7 November 2003)
Corresponding author R. L. Rasmusson: Department of Physiology and Biophysics, 124 Sherman Hall, State University of New York at Buffalo, Buffalo, NY 14214-3005, USA. Email: rr32@buffalo.edu

Kv1.4 is a member of the *Shaker*-related family of voltage-gated K^+ channels. The α-subunit of this channel is encoded by KCNA4. It produces a rapidly inactivating current, which is thought to be the molecular basis of the transient outward current seen in the endocardium of several mammalian species (Barry & Nerbonne, 1996). Hypertrophy and heart failure lead to up-regulation of Kv1.4 expression, indicating that the behaviour of this channel is of particular clinical importance (Lee *et al.* 1999; Kaprielian *et al.* 1999; Gidh-Jain *et al.* 1996; Nishiyama *et al.* 2001).

Kv1.4 channels inactivate by two distinct processes: N-type and C-type inactivation. N-type inactivation is rapid, and the molecular basis is well characterized: the NH_2 terminus of each subunit forms a 'ball', linked by a 'chain' to the transmembrane segments of the channel (Hoshi *et al.* 1990; Zagotta *et al.* 1990; Isacoff *et al.* 1991; Lopez *et al.* 1994; Holmgren *et al.* 1996; Jerng & Covarrubias, 1997). Channel activation involves a conformational change, which reveals a binding site for the N-terminal ball on the intracellular mouth of the pore. Binding of the ball has two physical consequences: occlusion of the permeation pathway, and a conformational change of both the channel and the ball subsequent to binding (Zhou *et al.* 2001). Occlusion of the permeation pathway has an immediate and direct effect, as current no longer flows. The conformational changes associated with, and subsequent to, binding of the N-terminal have less well-known consequences.

The molecular basis of C-type inactivation is controversial, but appears to involve changes at the selectivity filter, an extracellular conformational change, and intracellular pore closure. C-type inactivation is sensitive to extracellular permeant ions (Hoshi *et al.* 1991; Lopez-Barneo *et al.* 1993; Rasmusson *et al.* 1998), extracellular [TEA] (Armstrong, 1971; Choi *et al.* 1991;

© The Physiological Society 2003 DOI: 10.1113/jphysiol.2003.055012

Hoshi *et al.* 1991; Lipkind *et al.* 1995), intracellular quinidine binding (Wang *et al.* 2003), intracellular osmotic pressure changes (Jiang *et al.* 2003), mutations on the extracellular face of the channel near the mouth of the pore (Busch *et al.* 1991; Snyders & Chaudhary, 1996; Ficker *et al.* 1998) and mutations on the intracellular side of the pore (Li *et al.* 2003). In the absence of a concrete molecular basis, inactivation is described 'C-type' when it is exhibits most of the attributes outlined above, and in particular is insensitive to voltage and is slowed by an increase in $[K^+]_o$. Recovery from inactivation is controlled by the rate of recovery from C-type inactivation, regardless of the presence of N-type inactivation.

Even though N-type and C-type inactivation are distinct mechanisms which can be observed independently, they are coupled: C-type inactivation is speeded by the presence of N-type inactivation (Hoshi *et al.* 1991; Rasmusson *et al.* 1995; Baukrowitz & Yellen, 1995; Morales *et al.* 1996). Two mechanisms have been proposed to mediate this coupling: the 'permeation' and 'allosteric' mechanisms. The molecular basis of the permeation mechanism is that the reduction in K^+ ions at the extracellular mouth of the channel immediately following pore block is postulated to be large enough to have a significant effect on the rate of development of C-type inactivation. The allosteric hypothesis suggests the contribution from $[K^+]$ reduction following block will be functionally negligible compared to the contribution from allosteric mechanisms. Ion channels are contiguous proteins, even though they span the membrane, and the intra- and extracellular faces are usually exposed to markedly different ionic conditions. The molecular basis of the allosteric hypothesis is that conformational changes in the channel subsequent to N-terminal binding affect C-type inactivation. In this way, N- and C-type inactivation are coupled.

Previously, we have shown that a valine to alanine mutation on the intracellular side of S6 (see Fig. 1) disrupts C-type inactivation, and results in an anomalous speeding of C-type inactivation with high $[K^+]_o$ (Li *et al.* 2003). In 2 mM $[K^+]_o$, this mutation increases the rate of recovery from C-type inactivation. In this study, we show that more normal C-type inactivation behaviour can be restored to the mutant channel following binding of lipophilic moieties such as the N-terminal or quinidine to the intracellular pore mouth.

We propose that the valine to alanine mutation disrupts C-type inactivation by decreasing the structural stability of the open fKv1.4[V561A]ΔN channel. Binding of the N-terminal or quinidine to the intracellular mouth of the channel re-establishes the stability of the intracellular pore, and enables C-type inactivation to proceed normally. Our data suggest that the conformational state of S6 is important in the development of C-type inactivation. When lipophilic moieties bind to sites within the open pore they orientate S6, and promote a state which resembles the C-type inactivated state of the normal channel. This conformational change is the most likely explanation of the mechanism by which drug or N-terminal binding allosterically increases the rate of C-type inactivation in Kv1.4 channels. The reduction in $[K^+]_o$ following N-type inactivation may contribute to the coupling between N- and C-type inactivation, but under our experimental conditions this is not a major factor, and the allosteric mechanism predominates.

Methods

Mature female *Xenopus laevis* (Xenopus Express, Homosassa, FL, USA) were cared for according to standards approved by the Institutional Animal Care and Use Committee of the University at Buffalo SUNY. Frogs were anaesthetized by immersion in 1 g l^{-1} tricaine solution (Sigma). Oocytes were removed by partial ovariectomy and digested by placing them in a collagenase-containing Ca^{2+}-free OR2 solution (mM: 82.5 NaCl, 2 KCl, 1 $MgCl_2$, 5 Hepes; pH 7.4; 1 mg ml^{-1} collagenase, type I, Sigma). Frogs were killed humanely following final collection of oocytes. The oocytes were gently shaken for 1.5–2 h, with the enzyme solution refreshed at 1 h. Defolliculated oocytes (stage V–VI) were injected with up to 50 ng mRNA for a Kv1.4 clone isolated from ferret heart, fkv1.4 (Comer *et al.* 1994), using the Nanoject microinjection system (Drummond Scientific Co., Broomall, PA, USA). Mutations were made using the Stratagene Quickchange

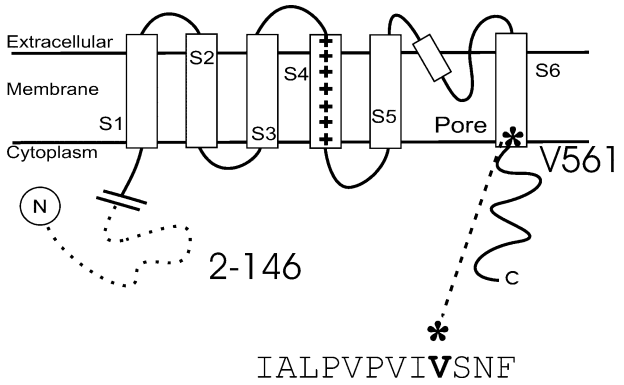

Figure 1. Schematic representation of the Kv1.4 channel
There are six transmembrane spanning domains, an N-terminal that forms a 'ball and chain' and a C-terminal. In the ΔN construct amino acids 2–146 are deleted, removing N-type inactivation. The position of a valine to alanine point mutation on the intracellular side of S6 is shown (Kv1.4[V561A]ΔN).

© The Physiological Society 2003

site-directed mutagenesis kit (Stratagene, Cedar Creek, TX, USA). A schematic diagram of the mutants and constructs used in this study is shown in Fig. 1.

Oocytes were voltage clamped in a whole cell mode configuration using a two-microelectrode oocyte clamp amplifier (CA-1B, Dagan Corp., Minneapolis, MN, USA), and currents were recorded at room temperature. Microelectrodes with resistances of 0.5–1.5 MΩ (when filled with 3 M KCl) were fabricated from 1.5 mm o.d. borosilicate glass tubing (TW150-4, World Precision Instruments, Sarasota, FL, USA) using a two-stage puller (Kopf Instruments, Tujunga, CA, USA) and filled with 3 M KCl. The control extracellular solution (2 mM K^+) contained (mM): 96 NaCl, 2 KCl, 1 $MgCl_2$, 1.8 $CaCl_2$, 10 Hepes, pH 7.4. The high potassium solution (98 mM K^+) contained (mM): 98 KCl, 1 $MgCl_2$, 1.8 $CaCl_2$, 10 Hepes, pH 7.4. Voltage clamp protocols used are described as appropriate in the text, and unless otherwise stated, raw two-electrode voltage clamp data traces were not leak or capacitance subtracted.

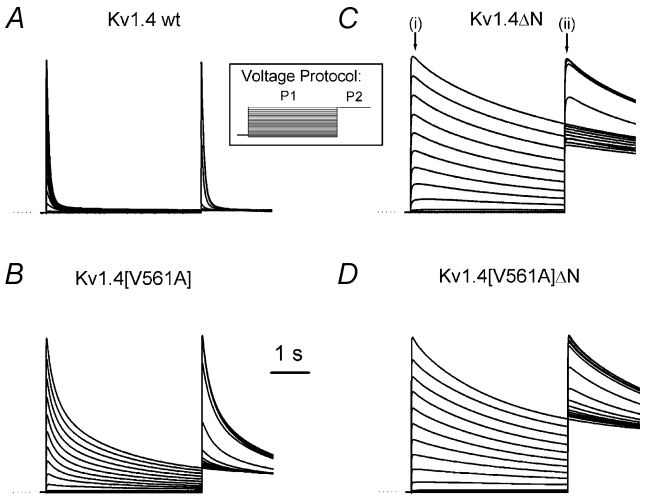

Figure 2. Representative current traces in response to a two-pulse steady state inactivation protocol
Channels were expressed in *Xenopus* oocytes and recorded with the two electrode voltage clamp technique. The initial 4 s pulse, P1, was to a voltage between –100 and +50 mV, in 10 mV steps. This was followed immediately by a 2 s pulse, P2, to +50 mV. The voltage protocol is shown in the inset. Currents are from: Kv1.4 wt (*A*); Kv1.4[V561A] (*B*); Kv1.4ΔN (*C*); and Kv1.4[V561A]ΔN (*D*). Currents are scaled so that the peak P1 current at +50 mV from each channel is the same size to allow comparisons. Dotted lines indicate zero current. The N-terminal-deleted currents exhibit the much slower C-type inactivation, whereas the inactivation of currents from N-terminal-intact channels are dominated by the much faster N-type inactivation. In *C*, (i) and (ii) indicate where the current–voltage and steady-state inactivation data were measured.

Data were digitized and analysed using pCLAMP 9.0 (Axon Instruments, Foster City, CA, USA). Further analysis was performed using Clampfit (Axon Instruments), Excel (Microsoft Corp) and Origin (Microcal Software Inc., Northampton, MA, USA). Data were filtered at 2 kHz. Data are shown as means ± S.E.M. Confidence levels were calculated using Student's paired *t* test or ANOVA as appropriate.

Results

Kv1.4 channels are voltage-gated K^+ channels with a putative structure of six transmembrane-spanning segments, including the charged voltage-sensing S4 segment. Figure 1 shows a schematic representation of the Kv1.4 channel and the position of mutations employed in this study. We used the two-electrode voltage clamp technique to study mutant and normal ferret Kv1.4 channels with and without the N-terminal [amino acids 2–146 are deleted] expressed in *Xenopus* ooctyes.

One of the defining characteristics of C-type inactivation is that an increase in $[K^+]_o$ results in a decrease in the rate at which C-type inactivation develops. However, a valine to alanine mutation on the intracellular side of the S6 transmembrane segment of the N-terminal-deleted Kv1.4 channel from ferrets results in a channel

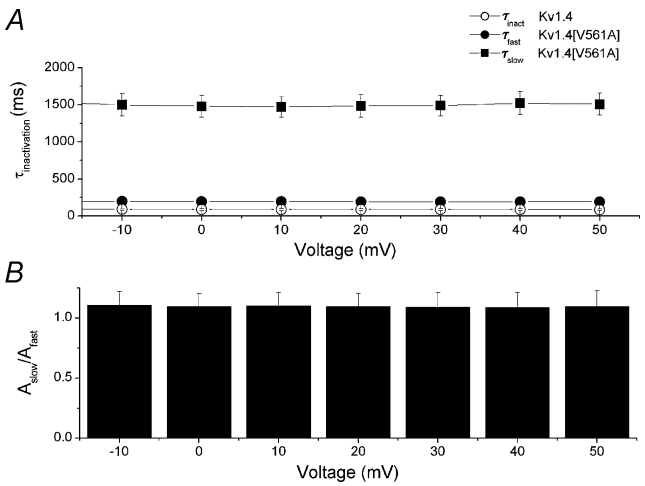

Figure 3. The V561A mutation alters the rate of inactivation for Kv1.4 channels with the N-terminal attached
A, inactivation of Kv1.4 channels is well fitted by a single exponential, and is voltage independent (○). The mean value of $\tau_{inactivation}$ over the range –10 to +50 mV is 103.24 ± 6.60 ms ($n = 6$). Inactivation of Kv1.4[V561A] channels is best fitted with a bi-exponential function. Over the range –10 to +50 mV mean τ_{fast} (●) is 191.95 ± 3.68 ms and mean τ_{slow} (■) is 1.493 ± 0.050 s ($n = 5$). *B*, the ratio of the amplitudes of the two Kv1.4[V561A] time constants is voltage independent. The mean ratio of the amplitudes of A_{slow}/A_{fast} is 1.095 ± 0.041 ($n = 5$) over the range –10 to +50 mV.

© The Physiological Society 2003

with an atypical relationship between C-type inactivation and $[K^+]_o$ (Li *et al.* 2003). Figure 2 shows typical voltage clamp current traces from the wild type fKv1.4 channel and the N-terminal-deleted channel, fKv1.4ΔN (amino acids 2–146 are deleted), and the corresponding channels with the valine to alanine mutation on the intracellular side of S6: fKv1.4[V561A] and fKv1.4[V561A]ΔN. There is little phenotypical difference between the N-terminal-deleted channels fKv1.4ΔN and fKv1.4[V561A]ΔN in the presence of 2 mM $[K^+]_o$ (Li *et al.* 2003). In contrast, N-terminal-intact fKv1.4[V561A] channels inactivate at a significantly slower rate than wild type Kv1.4 channels.

Inactivation of wild type Kv1.4 is best fitted by a single exponential, with $\tau_{inactivation} = 85.13 \pm 10.82$ ms at +50 mV ($n = 6$). There is no voltage sensitivity to $\tau_{inactivation}$ in the range 0 to +50 mV ($P > 0.999$, $n = 6$, ANOVA). Kv1.4[V561A] requires two exponentials for fitting: $\tau_{fast} = 200 \pm 12$ ms and $\tau_{slow} = 1630 \pm 139$ ms at +50 mV ($n = 6$). There is no voltage sensitivity to either τ_{fast} or τ_{slow} in the range 0 to +50 mV ($P > 0.999$, $n = 6$, ANOVA). The ratio of the amplitudes of the two Kv1.4[V561A] inactivation time constants, A_{slow}/A_{fast}, is 1.15 ± 0.13 ($n = 5$), which suggests that two processes make equal contributions to inactivation in this channel. There is no voltage sensitivity to A_{slow}/A_{fast} in the range 0 to +50 mV ($P = 1$, $n = 6$, ANOVA). Figure 3 shows the time constants of inactivation for Kv1.4 and Kv1.4[V561A] plotted against voltage, and the amplitude ratios for the two components of Kv1.4[V561A]. The fast component of inactivation of Kv1.4[V561A] is similar to the single inactivation component of Kv1.4, so it appears that the valine to alanine mutation has introduced a second inactivation time constant. However, there is a statistically significant difference between the fast time constant of inactivation of Kv1.4[V561A] and the time constant of inactivation of the wild type channel. Although these are not paired data, this difference may reflect a decrease in the availability of the fast N-terminal binding conformation, a decreased affinity of the channel for the N-terminal ball, or changes in some other processes.

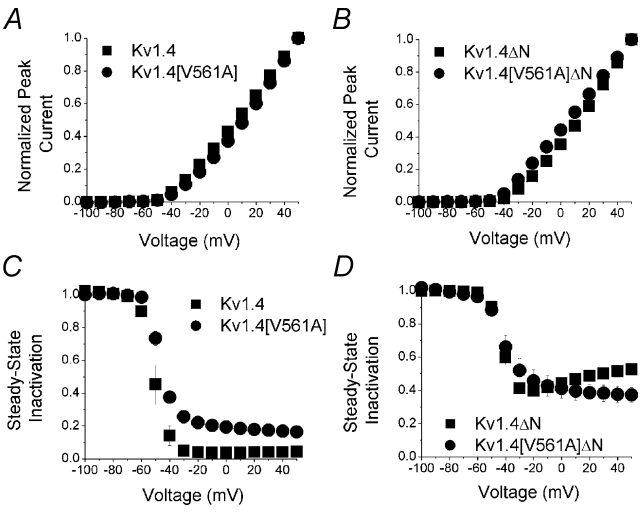

Figure 4. Current–voltage and steady-state inactivation relationships

Peak current elicited by the P1 pulse from the two pulse protocol (see Fig. 2*C*(i)) is plotted against voltage for *A*: Kv1.4 (■) and Kv1.4[V561A] (●) and *B*: Kv1.4ΔN (■) and Kv1.4[V561A]ΔN channels (●; $n = 5$, error bars are smaller than symbols). Steady-state inactivation relationships were determined from the two pulse protocol by calculating the ratio of the peak current in the P2 pulse (Fig. 2*C*(ii)) to the maximum value of the peak P1 current (Fig. 2*C*(i)). Steady-state inactivation relationships are shown for *C*: Kv1.4 (■) and Kv1.4[V561A] (●) and *D*: Kv1.4ΔN (■) and Kv1.4[V561A]ΔN channels (●; $n = 5$).

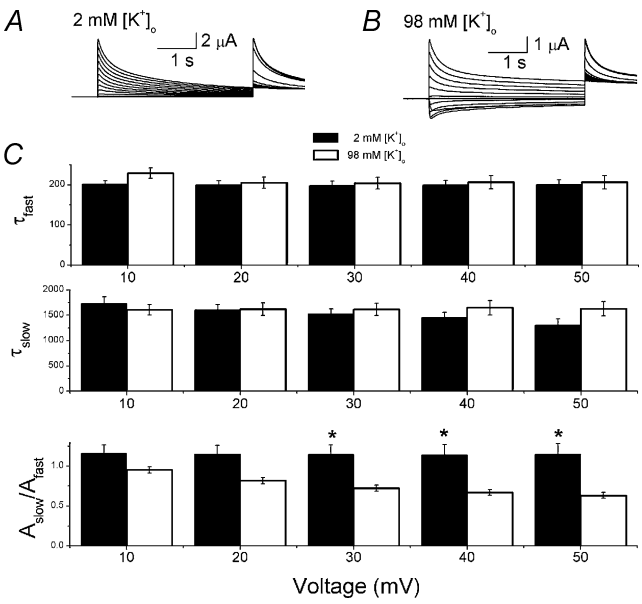

Figure 5. The effect of $[K^+]_o$ on the rate of inactivation of fKv1.4[V561A] channels

A and *B*, representative traces from a two pulse protocol (shown as inset of Fig. 2) on fKv1.4[V561A] channels at 2 mM $[K^+]_o$ (*A*) and 98 mM $[K^+]_o$ (*B*). Currents are scaled so that the peak of the P1 current elicited at +50 mV in both cases is the same size. *C*, inactivation of Kv1.4[V561A] channels is best fitted with a bi-exponential function. Changing $[K^+]_o$ from 2 (filled bar) to 98 mM (open bar) has little effect on the fast time constant, τ_{fast} (upper panel), or the slow time constant, τ_{fast} (middle panel), of inactivation of Kv1.4[V561A] channels. Over the range +10 to +50 mV, τ_{fast} is 199.73 ± 4.42 ms ($n = 5$) in 2 mM $[K^+]_o$ and 210.11 ± 6.49 ms ($n = 5$) in 98 mM $[K^+]_o$. Over the range +10 to +50 mV, τ_{slow} is 1.623 ± 0.052 s ($n = 5$) in 2 mM $[K^+]_o$ and 1.523 ± 0.055 s ($n = 5$) in 98 mM $[K^+]_o$. The ratio of the amplitudes of the two time constants, A_{slow}/A_{fast} is significantly affected by changing $[K^+]_o$ (bottom panel, significant differences denoted by asterisks, $P < 0.01$). Over the range +10 to +50 mV, in 2 mM $[K^+]_o$ A_{slow}/A_{fast} is 1.147 ± 0.050, and in 98 mM $[K^+]_o$ A_{slow}/A_{fast} is 0.759 ± 0.028 ($n = 5$, $P < 0.001$).

© The Physiological Society 2003

These changes may also be responsible for the persistent Kv1.4[V561A] current observed at the end of the P1 pulse in Fig. 2*B*.

There are few phenotypical changes in other basic biophysical properties of the mutant and normal constructs of Kv1.4. Figure 4 shows that the peak current–voltage relationships for all four channels are similar (Fig. 4*A* and *C*), as are the steady-state inactivation relationships (Fig. 4*B* and *D*), as determined by a two-pulse protocol.

N-type inactivation is insensitive to $[K^+]_o$. In contrast, sensitivity to $[K^+]_o$ is one of the defining characteristics of C-type inactivation. We have already shown that the relationship between the rate of inactivation in Kv1.4[V561]ΔN and $[K^+]_o$ is inverted, with an increase in $[K^+]_o$ resulting in an increase the rate of inactivation (Li *et al.* 2003). As noted above, inactivation of Kv1.4[V561A] is best fitted with two voltage-insensitive time constants. We looked at the relationship between $[K^+]_o$ and the rate of inactivation of Kv1.4[V561]. In paired data from 2 and 98 mM $[K^+]_o$ at +50 mV, The fast component of inactivation was not significantly affected by $[K^+]_o$ ($\tau_{fast,2K} = 200 \pm 12$ ms, $\tau_{fast,98K} = 206 \pm 17$ ms, $n = 5$). Raising $[K^+]_o$ resulted in a slight decrease in the slow component of inactivation at +50 mV, from $\tau_{slow,2K} = 1.630 \pm 0.139$ s, to $\tau_{slow,98K} = 1.307 \pm 0.120$ s ($n = 5$). The presence of 98 mM $[K^+]_o$ introduced a mild voltage dependence to the slow component of inactivation of Kv1.4[V561A]. The most significant $[K^+]_o$-sensitive property was the relative contribution of the two time constants. In the presence of 2 mM $[K^+]_o$ the contributions of τ_{fast} and τ_{slow} were approximately equal as the ratio of the amplitudes was close to 1: $A_{slow}/A_{fast} = 1.15 \pm 0.13$ ($n = 5$). When $[K^+]_o$ was raised to 98 mM τ_{fast} played a more dominant role, with the ratio A_{slow}/A_{fast} falling to 0.63 ± 0.04 at + 50 mV ($n = 5$). A slight voltage dependence to the ratio was apparent at high $[K^+]_o$ (Fig. 5). These results demonstrate that potassium has no effect on the time constants of inactivation of Kv1.4[V561A], but does affect the relative amplitude of the components.

The rate of recovery from inactivation in Kv1.4 channels is governed by recovery from C-type inactivation (Rasmusson *et al.* 1998). We measured recovery from inactivation using a standard gapped pulse protocol with a variable interstimulus interval. The ratio of the magnitude of the first and second pulse peak currents was used as an indication of the degree of recovery from inactivation.

Figure 6 shows the fraction of channels recovered plotted against the interstimulus interval. In the presence of 2 mM $[K^+]_o$ there is little difference in the rate of recovery from inactivation between wild type Kv1.4 and Kv1.4[V561A] channels (Fig. 6*A*), but there is a dramatic increase in

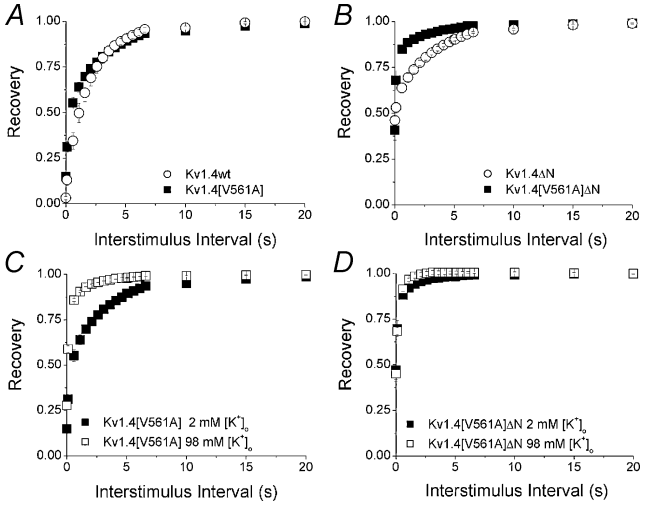

Figure 6. Recovery from Inactivation
Recovery from inactivation was measured using a standard variable interval gapped pulse protocol. An initial 5 s pulse (P1) from –90 to +50 mV was followed by a second pulse (P2) after an interval of between 0.1 and 20 s. The ratio of the peak current elicited by the P1 and P2 pulses ($I_{peak,P2}/I_{peak,P1}$)is plotted against pulse interval to show the recovery from inactivation. *A*, recovery curves for Kv1.4 (γ) and Kv1.4[V561A] (■) in 2 mM $[K^+]_o$. *B*, recovery curves for Kv1.4ΔN (γ) and Kv1.4[V561A]ΔN (■) in 2 mM $[K^+]_o$. Relationship between $[K^+]_o$ and recovery from inactivation of the mutant channels was measured using the same protocol. *C*, recovery from inactivation of Kv1.4[V561A] in 2 (■) and 98 mm $[K^+]_o$ (□). *D*, recovery from inactivation of Kv1.4[V561A]ΔN in 2 (■) and 98 mm $[K^+]_o$ (□).

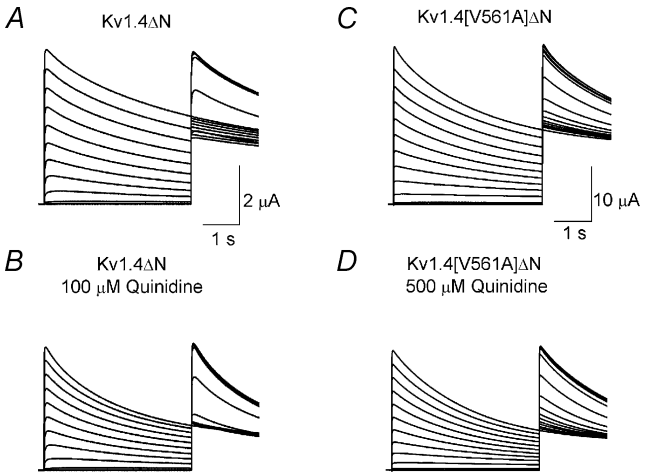

Figure 7. Representative traces showing the effect of quinidine on a channel undergoing a two pulse steady-state inactivation protocol (as described in Fig. 2)
A, control traces from Kv1.4ΔN. *B*, Kv1.4ΔN with 100 μM quinidine. *C*, Kv1.4[V561A]ΔN. *D*, Kv1.4[V561A]ΔN in the presence of 500 μM quinidine. In both cases, quinidine depressed the peak open current and speeded the rate of inactivation. Dotted lines indicate zero current.

© The Physiological Society 2003

the rate of recovery of Kv1.4[V561A]ΔN compared to Kv1.4ΔN channels (Fig. 6*B*). We next looked at the relationship between $[K^+]_o$ and the rate of recovery of the mutant from inactivation. There is a clear increase in the rate of recovery from inactivation of Kv1.4[V561A] (Fig. 6*C*) when $[K^+]_o$ is switched from 2 to 98 mM. This is similar to the behaviour of Kv1.4 wt channels when $[K^+]_o$ is switched from 2 to 98 mM (Li *et al.* 2003). The rate of recovery of Kv1.4[V561A]ΔN channels from inactivation is rapid in 2 mM $[K^+]_o$, and slightly more rapid with 98 mM $[K^+]_o$. Conversely, the effect of $[K^+]_o$ on Kv1.4ΔN channels is clearly seen, with the rate of recovery increasing with an increase in $[K^+]_o$ (Li *et al.* 2003; Fig. 6*D*). These results show that the characteristics of recovery from inactivation in Kv1.4[V561A] channels are similar to wild type, whereas recovery from inactivation is significantly altered in Kv1.4[V561A]ΔN channels. This suggests that the presence of the N-terminal reduces the effect of the valine to alanine mutation.

Quinidine is an open channel blocker which rapidly binds to the intracellular face of Kv1.4ΔN channels and occludes the pore (Wang *et al.* 2003). We looked at the effect of quinidine on Kv1.4[V561A]ΔN channels. Representative traces from a two-electrode double pulse protocol are shown in Fig. 7. The effects of quinidine on Kv1.4[V561A]ΔN and Kv1.4ΔN channels are qualitatively similar: it suppress the peak current and increases the rate of inactivation. However, the concentration of quinidine required to elicit an effect on Kv1.4[V561A]ΔN is much greater than that needed to elicit an equal effect on Kv1.4ΔN channels. This shows that the mutation has altered the effects of quinidine binding to the channel.

Figure 8 shows dose–response curves for peak current inhibition of Kv1.4[V561A]ΔN and Kv1.4ΔN by quinidine. The peak Kv1.4ΔN current is reduced to 50% by 106 mM quinidine, whereas the equivalent reduction in Kv1.4[V561A]ΔN current requires 611 mM quinidine.

Next, we looked at how the rate of recovery from inactivation was affected by quinidine. Previously, we have shown that the rate of recovery of Kv1.4ΔN from inactivation is not affected by the presence of quindine (Wang *et al.* 2003). Recovery from inactivation was measured using a standard variable interval gapped pulse protocol. The ratio of the magnitude of the first and second pulse peak currents was used as an indication of the degree of recovery from inactivation. The envelope of peak ratios was best fitted with a bi-exponential function. We looked at the effect of quinidine on the rate of recovery from inactivation. All data series were well fitted with a bi-exponential function (Table 1A). There was little difference in either the fast or slow time constants for the rate of recovery from inactivation in fKv1.4ΔN, fKv1.4[V561A], and fKv1.4[V561A]ΔN with 0, 500 μM or 1 mM quinidine. There was, however, a significant change in the amplitude ratios of the two components. The ratio of the amplitudes indicate that recovery in fKv1.4ΔN is dominated by the slow time constant. In

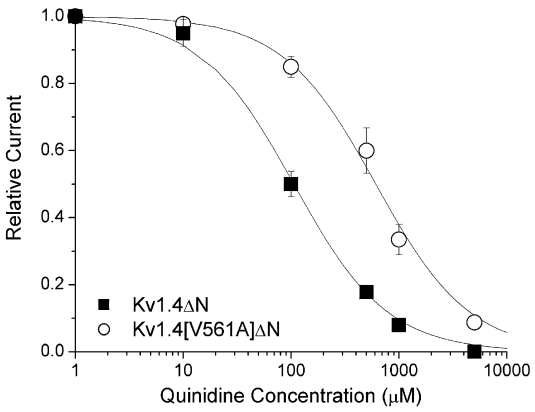

Figure 8. Dose–response curve for quinidine
The binding of quinidine to Kv1.4 ΔN (■) and Kv1.4[V561A]ΔN (○) in 2 mM $[K^+]_o$. Continuous lines are from a fit of the relationship $f = K_D/(K_D + [D])$, where f is fractional current, K_D is the apparent dissociation constant, and [D] is the quinidine concentration. Using this relationship, Kv1.4ΔN current was reduced to 50% by 106 mM quinidine, but 611 mM quinidine was required to reduce Kv1.4[V561A]ΔN by 50%.

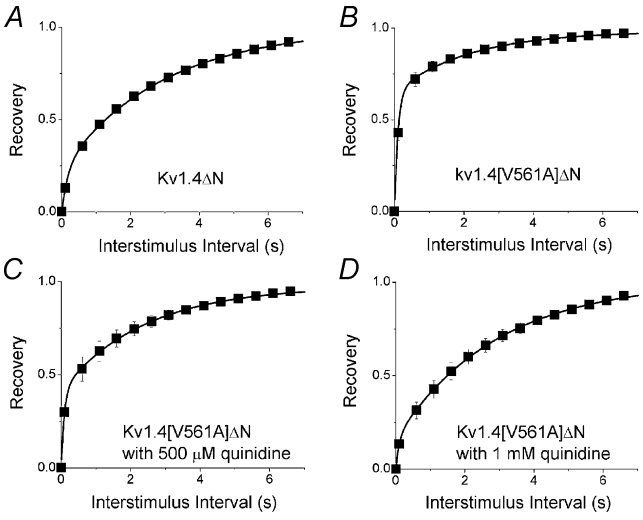

Figure 9. Recovery from inactivation fitted with a bi-exponential function
All channels were well fitted with a bi-exponential function, with the following values: fKv1.4ΔN: $\tau_{recover,fast} = 0.21 \pm 0.04$ s, $\tau_{recover,slow} = 2.94 \pm 0.15$ s ($n = 7$); fKv1.4[V561A]ΔN: $\tau_{recover,fast} = 0.11 \pm 0.02$ s, $\tau_{recover,slow} = 2.41 \pm 0.14$ s ($n = 9$); fKv1.4[V561A]ΔN with 500 μM quinidine: $\tau_{recover,fast} = 0.12 \pm 0.01$ s, $\tau_{recover,slow} = 2.64 \pm 0.22$ s ($n = 7$); fKv1.4[V561A]ΔN with 1 mM quinidine: $\tau_{recover,fast} = 0.03 \pm 0.01$ s, $\tau_{recover,slow} = 2.81 \pm 0.18$ s ($n = 7$).

© The Physiological Society 2003

Table 1. Time constants of inactivation and amplitude ratios obtained from fitting recovery from inactivation with a bi-exponential function

	$\tau_{recover,fast}$	$\tau_{recover,slow}$	A_{fast}/A_{slow}	n
A. Fitted time constants				
fKv1.4 ΔN	0.21 ± 0.04 s	2.94 ± 0.15 s	0.33 ± 0.05	7
fKv1.4[V561A]ΔN	0.11 ± 0.02 s	2.41 ± 0.14 s	2.40 ± 0.37	7
fKv1.4[V561A]ΔN + 500 μM quinidine	0.12 ± 0.01 s	2.64 ± 0.22 s	0.98 ± 0.27	7
fKv1.4[V561A]ΔN + 1 mM quinidine	0.03 ± 0.01 s	2.81 ± 0.18 s	0.22 ± 0.10	7
B. Fixed time constants				
fKv1.4 ΔN:	0.12 s	2.70 s	0.28 ± 0.06	7
fKv1.4[V561A]ΔN	0.12 s	2.70 s	2.85 ± 0.54	7
fKv1.4[V561A]ΔN + 500 μM quinidine	0.12 s	2.70 s	1.03 ± 0.26	7
fKv1.4[V561A]ΔN + 1 mM quinidine	0.12 s	2.70 s	0.27 ± 0.10	7

contrast, fKv1.4[V561A]ΔN recovery is dominated by the fast time constant. The presence of 500 μM quinidine decreases the ratio of the amplitudes. The addition of 1 mM quinidine further reduced the ratio of the amplitudes, giving a value similar to the unmutated channel, with the slow component dominating once more. These data show that recovery from inactivation is very different in fKv1.4ΔN and fKv1.4[V561A]ΔN channels. However, the addition of 1 mM quinidine reduces the effect of the valine to alanine mutation.

The fast and slow time constants for all the data presented in Fig. 10 were similar, but not identical. We therefore reanalysed the data using fixed time constants. The mean values of the two rate constants for a bi-exponential fit to all the data from fKv1.4 ΔN, fKv1.4[V561A]ΔN, fKv1.4[V561A]ΔN with 500 μM quinidine, and fKv1.4[V561A]ΔN with 1 mM quinidine were $\tau_{recover,slow} = 2.70 \pm 0.11$ s and $\tau_{recover,fast} = 0.12 \pm 0.04$ s. We used these as fixed time constants to reanalyse the data, and measure the ratio of amplitudes (Table 1B). There was a significant difference between the ratio of the amplitudes for fKv1.4ΔN and fKv1.4[V561A]ΔN ($n = 7$, $P < 0.01$) but there was no significant difference between the ratio of the amplitudes for fKv1.4ΔN and fKv1.4[V561A]ΔN with 1 mM quinidine.

We next investigated whether the ability of quinidine to suppress current was affected by $[K^+]_o$. We have shown previously that increasing $[K^+]_o$ from 2 to 98 mM reduces the effectiveness of quinidine to suppress fKv1.4ΔN (Wang *et al.* 2003). Figure 8 shows that 50% reduction of current is achieved with ∼100 μM for fKv1.4[V561A]ΔN and ∼1 mM for fKv1.4[V561A]ΔN. We therefore compared the current suppression at these two concentrations for the respective channels. When fKv1.4ΔN channels were constantly exposed to 100 μM quinidine but $[K^+]_o$ was switched from 2 to 98 mM, there was a reduction in the ability of quinidine to inhibit the current at +50 mV. fKv1.4ΔN currents in 100 μM quinidine and 98 mM $[K^+]_o$ were 124 ± 12% of those observed in 100 μM quinidine and 2 mM $[K^+]_o$ ($n = 4$). In contrast, the ability of quinidine to inhibit fKv1.4[V561A]ΔN current at +50 mV was independent of $[K^+]_o$: fKv1.4[V561A]ΔN currents with 1 mM quinidine and 98 mM $[K^+]_o$ were similar (101 ± 11%) to those observed with 1 mM quinidine and 2 mM $[K^+]_o$ ($n = 5$). The valine to alanine mutation reduced the ability of $[K^+]_o$ to interfere with quinidine binding.

Increasing $[K^+]_o$ reduces the rate of inactivation of fKv1.4ΔN channels, but increases the rate of inactivation of fKv1.4[V561A]ΔN channels (Li *et al.* 2003). We looked at the relationship between inactivation and $[K^+]_o$ in the presence of quinidine. Switching from 2 to 98 mM $[K^+]_o$ in fKv1.4[V561A]ΔN channels increased the rate of inactivation from 2.16 ± 0.14 to 1.53 ± 0.07 s ($n = 6$). Addition of 1 mM quinidine increased the rate of inactivation of fKv1.4[V561A]ΔN channels in both 2 and 98 mM $[K^+]_o$. In the presence of 2 mM $[K^+]_o$ and 1 mM quinidine, $\tau_{inactivation}$ was 79.0 ± 4.3% of control values. This is similar to the results obtained with 98 mM $[K^+]_o$ and 1 mM quinidine: $\tau_{inactivation}$ in the presence of 98 mM $[K^+]_o$ and 1 mM quinidine was 84.8 ± 2.8% of the control inactivation in 98 mM $[K^+]_o$ ($n = 6$). This is shown in Fig. 11. These data demonstrate that extracellular depletion of $[K^+]_o$ is not involved in the ability of quinidine to enhance C-type inactivation.

Discussion

Inactivation is an important determinant of ion channel function. Even minor alterations in the inactivation or recovery of a channel, such as those identified as the molecular basis of episodic ataxia (Adelman *et al.* 1995), can result in considerable deleterious consequences. The development of inactivation during a depolarizing pulse

© The Physiological Society 2003

(e.g. an action potential) is critical to normal physiological function, e.g. repolarization. Recovery from inactivation is equally important, as it determines channel participation in subsequent action potentials.

There are a number of similarities between ion channel inactivation and open channel block (Armstrong, 1966, 1968, 1969; Demo & Yellen, 1991). Fast inactivation of *Shaker* K^+ channels results from the binding of a positively charged lipophilic portion of the N-terminal domain to the open channel (Aldrich *et al.* 1990; Zagotta *et al.* 1990; Hoshi *et al.* 1990, 1991). This mechanism was subsequently demonstrated in several other K^+ channels (for review see Rasmusson *et al.* 1998). The similarity between N-type inactivation and intracellularly acting open channel blockers was immediately apparent. Most open channel K^+ channel blockers have a positively charged nitrogen group, but are otherwise generally lipophilic. The receptor site for both drug and N-terminal binding has been localized to residues on the cytoplasmic side of S6 (Lopez *et al.* 1994; Yeola *et al.* 1996).

For many ion channels, inactivation persists even in the absence of the N-terminal 'ball' domain. The molecular basis of this second or 'slow' inactivation is controversial, and is generally labelled C-type inactivation. C-type inactivation is competitively inhibited by $[TEA^+]_o$ or $[K^+]_o$ (Heginbotham & MacKinnon, 1992; Lopez-Barneo *et al.* 1993), and modulated by a series of mutations at the extracellular mouth of the channel (Hoshi *et al.* 1991; Lopez-Barneo *et al.* 1993; Liu *et al.* 1996). Channels with intact N-terminal domains but mutations that inhibit C-type inactivation inactivate via the N-type inactivation. Almost paradoxically, recovery from inactivation in these channels is governed by the properties of recovery from C-type inactivation, even though in the absence of the N-terminal, C-type inactivation had developed extremely slowly (Hoshi *et al.* 1991). It was therefore concluded that N-type inactivation promoted or catalysed the development of C-type inactivation, a finding which was subsequently generalized to drug binding (Baukrowitz & Yellen, 1996) and other channel types (Rasmusson *et al.* 1995).

This paper examines the properties of coupling between N-type inactivation or quinidine binding and the C-type inactivation process. There are two main hypotheses concerning the link between occlusion

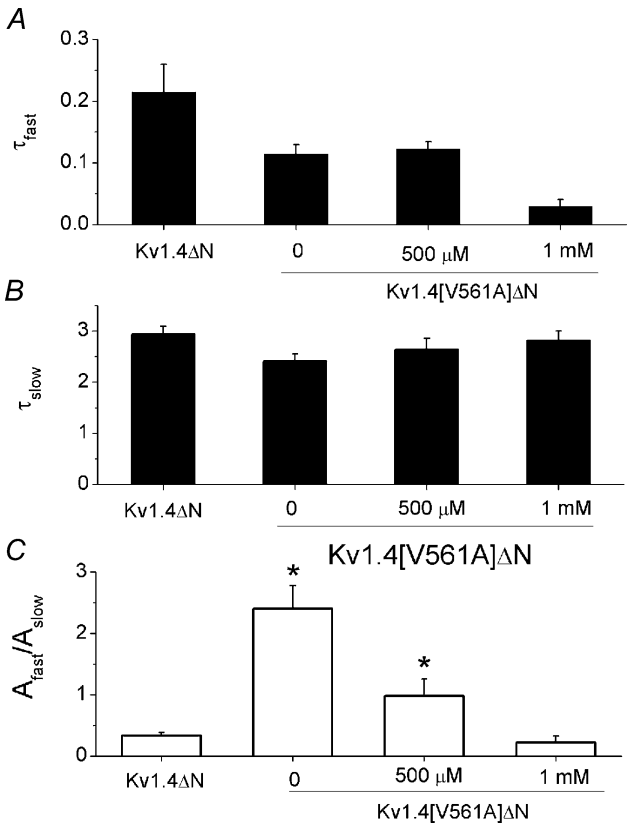

Figure 10. Comparison of recovery rates data from fKv1.4ΔN without quinidine, and fKv1.4[V561A]ΔN with 0, 500 μm or 1 mm quinidine

A, the fast rate of recovery from inactivation. *B*, the slow rate of recovery. *C*, the ratio of the amplitude of the fast and slow rate constants, A_{fast}/A_{slow}. The slow time constant dominates recovery in fKv1.4ΔN channels (no quinidine present, $A_{fast}/A_{slow} = 0.33 \pm 0.05$), and the fast time constant dominates fKv1.4[V561A] recovery from inactivation (no quinidine present, $A_{fast}/A_{slow} = 2.40 \pm 0.37$). In the presence of 500 μM quinidine the amplitude ratio of fKv1.4[V561A]ΔN recovery is close to 1 ($A_{fast}/A_{slow} = 0.98 \pm 0.27$), and in the presence of 1 mM quinidine the ratio of the time constants in fKv1.4[V561A]ΔN ($A_{fast}/A_{slow} = 0.22 \pm 0.10$) reverts to a ratio similar to that found in the unmutated fKv1.4ΔN construct. Significant differences from fKv1.4ΔN data are denoted by asterisks ($P < 0.01$).

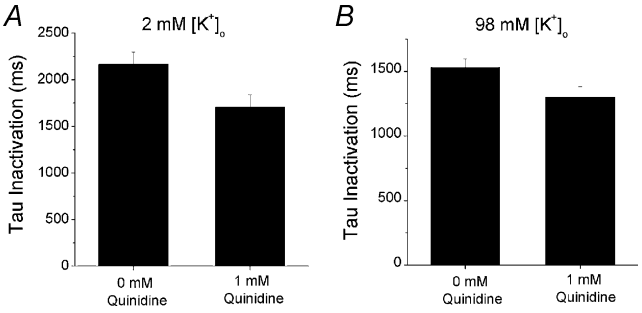

Figure 11. The ability of quinidine to increase the rate of inactivation in fKv1.4[V561A]ΔN channels is $[K^+]_o$ independent

A, in the presence of 2 mM $[K^+]_o$, $\tau_{inactivation,2K} = 2.164 \pm 0.135$ s. Addition of 1 mM quinidine increases the rate of inactivation to $\tau_{inactivation,2K,1mMQ} = 1.706 \pm 0.132$ s. *B*, in the presence of 98 mM $[K^+]_o$, $\tau_{inactivation,98K} = 1.529 \pm 0.066$. The addition of 1 mM quinidine further increases the rate of inactivation: $\tau_{inactivation,98K,1mMQ} = 1.300 \pm 0.079$ s.

© The Physiological Society 2003

of the intracellular pore by drug or lipophilic peptides and the coupling to C-type inactivation: the 'permeation' mechanism and the 'allosteric' mechanism. The permeation mechanism (Baukrowitz & Yellen, 1996) is based on the idea that blocking K^+ permeation directly effects C-type inactivation. Normally, high K^+ ion flux results in local accumulation of $[K^+]_o$ due to unstirred layer effects. Occlusion of the permeation pathway, by N-type inactivation or drug binding, decreases $[K^+]$ near the extracellular vestibule. Since extracellular K^+ slows C-type inactivation, the reduction in $[K^+]_o$ means there is no 'foot in the door' hindering the channel from adopting the C-type inactivated state (Baukrowitz & Yellen, 1995, 1996). The allosteric mechanism (Wang *et al.* 1997*b*; Ficker *et al.* 1998) proposes that the effect of reducing the K^+ accumulation is negligible compared to the contribution from a direct physical interaction between events at the intracellular pore and C-type inactivation, which are mediated by the channel protein.

C-type inactivation involves a conformational change at the extracellular mouth of the pore (Rasmusson *et al.* 1998). However, considerable evidence is emerging to indicate that C-type inactivation also involves major conformational changes on the intracellular side of the channel. We have shown that C-type inactivation in Kv1.4 channels involves a significant conformational change at the intracellular side of the pore (Jiang *et al.* 2003). This pore closure mechanism is consistent with earlier reports by other groups that C-type inactivation prevents the intracellular binding of 4-aminopyridine in Kv channels (Castle *et al.* 1994) and dofetilide in HERG (Ficker *et al.* 1998). Furthermore, intracellular mutations on the S6 transmembrane spanning domain can have a major impact on the development and recovery of C-type inactivation (Adelman *et al.* 1995; Chen *et al.* 2002; Li *et al.* 2003).

The V561A mutation used in this study alters C-type inactivation in Kv1.1 and N-terminal-deleted Kv1.4 channels (Adelman *et al.* 1995; Li *et al.* 2003). Perhaps most importantly, this mutant reverses the relationship between $[K^+]_o$ and C-type inactivation. Instead of slowing C-type inactivation, increasing $[K^+]_o$ speeded development of inactivation. The reversal of the $[K^+]_o$ sensitivity of this phenotype made this mutant channel an ideal for testing the permeation hypothesis. Figure 11 shows that quinidine binding increases the apparent rate of fKv1.4[V561A]ΔN inactivation. If the permeation mechanism plays a significant role in modulating C-type inactivation, then quinidine block should slow the apparent rate of development of C-type inactivation in fKv1.4[V561A]ΔN, due to local $[K^+]$ depletion. However, the exact opposite is true: quinidine binding to fKv1.4[V561A]ΔN promotes development of a C-type inactivated state. Furthermore, the apparent increase in the inactivation rate caused by increasing $[K^+]_o$ from 2 to 98 mM was still present when applied in the presence of quinidine. This finding cannot be reconciled with the permeation hypothesis. This suggests that allosteric mechanisms dominate coupling in fKv1.4[V561A]ΔN channels, and, by extension, may dominate in the wild type channel.

What is the nature of the allosteric interaction? S6 movement seems to be an important component of the mechanism. Mutations at both the cytoplasmic and extracellular ends of S6 strongly modulate the properties of C-type inactivation (Claydon *et al.* 2000; Li *et al.* 2003). K^+ channel X-ray crystallography studies in the presence of the N-terminal peptide predict significant interactions between the cytoplasmic side of S6 and N-type inactivation (Zhou *et al.* 2001). The side-chains that interact with potassium channel blockers have been mapped to the same region of S6 (Yeola *et al.* 1996; Caballero *et al.* 2002). In HERG channels, mutations and manipulations which inhibit C-type inactivation lower the affinity of the channels for methanesulphonanilide compounds such as E-4031 and dofetilide (Wang *et al.* 1997*b*; Ficker *et al.* 2001). In HERG, the ability of a variety of drugs (e.g. dofetilide, MK-499, cisapride, terfenadine, chloroquine, quinidine) to bind is critically dependent on positioning of specific aromatic residues on S6 (Mitcheson *et al.* 2000; Chen *et al.* 2002; Sanchez-Chapula *et al.* 2002) and S6 rotation may be an important step in binding (Chen *et al.* 2002).

Development of C-type inactivation HERG is extremely rapid, as is recovery from inactivation (of the order of ms: Sanguinetti *et al.* 1995; Kiehn *et al.* 1996; Wang *et al.* 1997*a*; Bett & Rasmusson, 2003), making generalization of the S6 rotation hypothesis to the more distantly related Kv channels questionable. Development of, and recovery from, C-type inactivation in Kv channels typically occurs in the range of hundreds of milliseconds to seconds (Rasmusson *et al.* 1998). Interventions from the extracellular side of the pore mouth which reduce C-type inactivation (either through mutation or application of high $[K^+]_o$) have in general reduced the affinity of drugs in parallel with the reduction of C-type inactivation (Wang *et al.* 1997*b*, 2003; Ficker *et al.* 2001). Similarly, the ability of a drug to increase the rate of development of C-type inactivation is dependent on the affinity of the open channel for drug.

If the binding of quinidine to Kv1.4ΔN channels is dependent on the orientation and lipophilic balance of the S6 transmembrane domain, then introduction of

© The Physiological Society 2003

a lipophilic moiety such as an N-terminal domain or open-channel blocking drugs such as quinidine will change the hydration energy of the pore-lining domains. We propose that the link between C-type inactivation and drug or N-terminal domain binding involves rotation of S6. This leads to two important predictions for intracellularly acting drugs which promote development of C-type inactivation. First, manipulations on the extracellular face of the channel which inhibit C-type inactivation will also lower drug binding affinity. This has been demonstrated previously (Wang *et al.* 1997*b*, 2003; Ficker *et al.* 2001). Second, certain mutations on the intracellular side of S6 should be able to change drug affinity independently of the ability to promote C-type inactivation. That is one of the important consequences of this study. The fKv1.4[V561A]ΔN channel has a dramatically reduced affinity for quinidine compared to fKv1.4ΔN (611 and 106 mM, respectively), but quinidine binding retains the ability to induce C-type inactivation. The reduction in affinity is similar to that seen for inhibition of C-type inactivation by 98 mM $[K^+]_o$ or the K532Y mutation on the extracellular face of the channel, but both of these extracellular manipulations also abolish the ability to promote C-type inactivation (Wang *et al.* 2003). Thus, our results fit the predictions of the S6 rotational model proposed for HERG (Chen *et al.* 2002), but do not distinguish between rotation and other conformational changes of S6.

Other results can also be explained within the context of this putative involvement of S6 in channel gating, drug binding and development of C-type inactivation. One is the prediction that S6 moves in the open state and is sensitive to the balance of water and hydrophobic elements within the inner vestibule and to $[K^+]_o$. The conformation of S6 should be critical to binding of the N-terminal domain. N-type inactivation was slowed relative to the wild type channel in the fKv1.4[V561A] channel, which has an intact N-terminal. The slowing of inactivation may be due to a reduction in the availability of a high affinity binding conformation for lipophilic moieties. This could also explain the bi-exponential nature of the inactivation. More importantly, increasing $[K^+]_o$ increases the relative amplitude of the fast component of fKv1.4[V561A] N-type inactivation. N-type inactivation is unaffected by $[K^+]_o$, but C-type inactivation in fKv1.4[V561A]ΔN is promoted by an increase in $[K^+]_o$. This is consistent with the idea that binding by lipophilic moieties is linked to C-type inactivation through the conformation of S6.

We can also gain some insight into the final inactivated state or states which the channel enters by examining the process of recovery from inactivation. Recovery from inactivation is similar for fKv1.4 and fKv1.4[V561A] channels, but the fKv1.4[V561A]ΔN channel recovers much quicker than the fKv1.4ΔN channel. Recovery from inactivation in fKv1.4[V561A]ΔN is a bi-exponential process, with an initial dominant rapid recovery, accompanied by a small amplitude slow recovery with a time constant similar to that of C-type inactivation in fKv1.4ΔN or wild type fKv1.4. This is consistent with there being two C-type inactivated states of this channel, a short lived, rapidly recovering state and a stable slowly recovering inactivated state. The balance between these two states should be influenced by binding of the N-terminal domain. Our results clearly show that the presence of the N-terminal domain results in a time course of recovery of the V561A channel which is consistent with both the slow component of the N-terminal-deleted mutant channel and with an N-terminal-intact wild type Kv1.4 channel.

This effect of lipophilic mechanism was tested in more detail using varying levels of quinidine. As shown in Fig. 10, the balance between fast and slow components of recovery in the fKv1.4[V561A]ΔN channel was a direct function of the concentration of quinidine. The more quinidine, the larger the relative amplitude of the slow component of recovery. Even though there is little structural similarity between quinidine and the N-terminal ball domain, the presence of either slows rapid fKv1.4[V561A]ΔN channel recovery to match the rate of recovery of the wild type channel.

We suggest that our findings can be explained by the action of lipophilic moieties within the pore that orientate S6 and cause a conformational change to a bound state which resembles the C-type inactivated state of the normal channel. This conformational change is the likely mechanism by which drug binding allosterically increases the rate of C-type inactivation in Kv1.4 channels. Although the permeation mechanism may contribute to the coupling between N-type and C-type inactivation in some circumstances, its contribution is minimal under these experimental conditions.

References

Adelman JP, Bond CT, Pessia M & Maylie J (1995). Episodic ataxia results from voltage-dependent potassium channels with altered functions. *Neuron* **15**, 1449–1454.

Aldrich RW, Hoshi T & Zagotta WN (1990). Differences in gating among amino-terminal variants of Shaker potassium channels. *Cold Spring Harbor Symposia Quantitative Biol* **55**, 19–27.

© The Physiological Society 2003

Armstrong CM (1966). Time course of TEA^+-induced anomalous recification in squid giant axons. *J General Physiol* **50**, 491–503.

Armstrong CM (1968). Induced inactivation of the potassium permeability of squid axon membranes. *Nature* **219**, 1262–1263.

Armstrong CM (1969). Inactivation of the potassium conductance and related phenomena caused by quaternary ammonium ion injection in squid axons. *J General Physiol* **54**, 553–575.

Armstrong CM (1971). Interaction of tetraethylammonium ion derivatives with the potassium channels of giant axons. *J General Physiol* **58**, 413–437.

Barry DM & Nerbonne JM (1996). Myocardial potassium channels: electrophysiological and molecular diversity. *Ann Rev Physiol* **58**, 363–394.

Baukrowitz T & Yellen G (1995). Modulation of K^+ current by frequency and external $[K^+]$: a tale of two inactivation mechanisms. *Neuron* **15**, 951–960.

Baukrowitz T & Yellen G (1996). Two functionally distinct subsites for the binding of internal blockers to the pore of voltage-activated K^+ channels. *Proc Nat Acad Sci* **93**, 13357–13361.

Bett GCL & Rasmusson RL (2003). Functionally-distinct proton-binding in HERG suggests the presence of two binding sites. *Cell Biochem Biophys* **39**, 183–194.

Busch AE, Hurst RS, North RA, Adelman JP & Kavanaugh MP (1991). Current inactivation involves a histidine residue in the pore of the rat lymphocyte potassium channel RGK5. *Biochem Biophys Res Comm* **179**, 1384–1390.

Caballero R, Moreno I, Gonzalez T, Valenzuela C, Tamargo J & Delpon E (2002). Putative binding sites for benzocaine on a human cardiac cloned channel (Kv1.5). *Cardiovasc Res* **56**, 104–117.

Castle NA, Fadous SR, Logothetis DE & Wang GK (1994). 4-Aminopyridine binding and slow inactivation are mutually exclusive in rat Kv1.1 and Shaker potassium channels. *Mol Pharmacol* **46**, 1175–1181.

Chen J, Seebohm G & Sanguinetti MC (2002). Position of aromatic residues in the S6 domain, not inactivation, dictates cisapride sensitivity of HERG and eag potassium channels. *Proc Natl Acad Sci* **99**, 12461–12466.

Choi KL, Aldrich RW & Yellen G (1991). Tetraethylammonium blockade distinguishes two inactivation mechanisms in voltage-activated K^+ channels. *Proc Nat Acad Sci* **88**, 5092–5095.

Claydon TW, Boyett MR, Sivaprasadarao A, Ishii K, Owen JM, O'Beirne HA, Leach R, Komukai K & Orchard CH (2000). Inhibition of the K^+ channel kv1.4 by acidosis: protonation of an extracellular histidine slows the recovery from N-type inactivation. *J Physiol* **526**, 253–264.

Comer MB, Campbell DL, Rasmusson RL, Lamson DR, Morales MJ, Zhang Y & Strauss HC (1994). Cloning and characterization of an Ito-like potassium channel from ferret ventricle. *Am J Physiol* **267**, H1383–H1395.

Demo SD & Yellen G (1991). The inactivation gate of the Shaker K^+ channel behaves like an open-channel blocker. *Neuron* **7**, 743–753.

Ficker E, Jarolimek W & Brown AM (2001). Molecular determinants of inactivation and dofetilide block in ether a-go-go (EAG) channels and EAG-related K^+ channels. *Mol Pharmacol* **60**, 1343–1348.

Ficker E, Jarolimek W, Kiehn J, Baumann A & Brown AM (1998). Molecular determinants of dofetilide block of HERG K^+ channels. *Circ Res* **82**, 386–395.

Gidh-Jain M, Huang B, Jain P & El Sherif N (1996). Differential expression of voltage-gated K^+ channel genes in left ventricular remodeled myocardium after experimental myocardial infarction. *Circ Res* **79**, 669–675.

Heginbotham L & MacKinnon R (1992). The aromatic binding site for tetraethylammonium ion on potassium channels. *Neuron* **8**, 483–491.

Holmgren M, Jurman ME & Yellen G (1996). N-type inactivation and the S4–S5 region of the Shaker K^+ channel. *J General Physiol* **108**, 195–206.

Hoshi T, Zagotta WN & Aldrich RW (1990). Biophysical and molecular mechanisms of Shaker potassium channel inactivation. *Science* **250**, 533–538.

Hoshi T, Zagotta WN & Aldrich RW (1991). Two types of inactivation in Shaker K^+ channels: effects of alterations in the carboxy-terminal region. *Neuron* **7**, 547–556.

Isacoff EY, Jan YN & Jan LY (1991). Putative receptor for the cytoplasmic inactivation gate in the Shaker K^+ channel. *Nature* **353**, 86–90.

Jerng HH & Covarrubias M (1997). K^+ channel inactivation mediated by the concerted action of the cytoplasmic N- and C-terminal domains. *Biophys J* **72**, 163–174.

Jiang X, Bett GC, Li X, Bondarenko VE & Rasmusson RL (2003). C-type inactivation involves a significant decrease in the intracellular aqueous pore volume of Kv1.4 K^+ channels expressed in *Xenopus* oocytes. *J Physiol* **549**, 683–695.

Kaprielian R, Wickenden AD, Kassiri Z, Parker TG, Liu PP & Backx PH (1999). Relationship between K^+ channel down-regulation and $[Ca2^+]_i$ in rat ventricular myocytes following myocardial infarction. *J Physiol* **517**, 229–245.

Kiehn J, Lacerda AE, Wible B & Brown AM (1996). Molecular physiology and pharmacology of HERG. Single-channel currents and block by dofetilide. *Circulation* **94**, 2572–2579.

Lee JK, Nishiyama A, Kambe F, Seo H, Takeuchi S, Kamiya K, Kodama I & Toyama J (1999). Downregulation of voltage-gated K(+) channels in rat heart with right ventricular hypertrophy. *Am J Physiol* **277**, H1725–H1731.

Li X, Bett GC, Jiang X, Bondarenko VE, Morales MJ & Rasmusson RL (2003). Regulation of N- and C-type inactivation of Kv1.4 by pHo and K^+: evidence for transmembrane communication. *Am J Physiol)* **284**, H71–H80.

© The Physiological Society 2003

Lipkind GM, Hanck DA & Fozzard HA (1995). A structural motif for the voltage-gated potassium channel pore. *Proc Nat Acad Sci* **92**, 9215–9219.

Liu Y, Jurman ME & Yellen G (1996). Dynamic rearrangement of the outer mouth of a K^+ channel during gating. *Neuron* **16**, 859–867.

Lopez GA, Jan YN & Jan LY (1994). Evidence that the S6 segment of the Shaker voltage-gated K^+ channel comprises part of the pore. *Nature* **367**, 179–182.

Lopez-Barneo J, Hoshi T, Heinemann SH & Aldrich RW (1993). Effects of external cations and mutations in the pore region on C-type inactivation of Shaker potassium channels. *Receptors Channels* **1**, 61–71.

Mitcheson JS, Chen J, Lin M, Culberson C & Sanguinetti MC (2000). A structural basis for drug-induced long QT syndrome. *Proc Nat Acad Sci* **97**, 12329–12333.

Morales MJ, Wee JO, Wang S, Strauss HC & Rasmusson RL (1996). The N-terminal domain of a K^+ channel beta subunit increases the rate of C-type inactivation from the cytoplasmic side of the channel. *Proc Nat Acad Sci* **93**, 15119–15123.

Nishiyama A, Ishii DN, Backx PH, Pulford BE, Birks BR & Tamkun MM (2001). Altered K^+ channel gene expression in diabetic rat ventricle: isoform switching between Kv4.2 and Kv1.4. *Am J Physiol* **281**, H1800–H1807.

Rasmusson RL, Morales MJ, Castellino RC, Zhang Y, Campbell DL & Strauss HC (1995). C-type inactivation controls recovery in a fast inactivating cardiac K^+ channel (Kv1.4) expressed in *Xenopus* oocytes. *J Physiol* **489**, 709–721.

Rasmusson RL, Morales MJ, Wang S, Liu S, Campbell DL, Brahmajothi MV & Strauss HC (1998). Inactivation of voltage-gated cardiac K^+ channels. *Circ Res* **82**, 739–750.

Sanchez-Chapula JA, Navarro-Polanco RA, Culberson C, Chen J & Sanguinetti MC (2002). Molecular determinants of voltage-dependent human ether-a-go-go related gene (HERG) K^+ channel block. *J Biol Chem* **277**, 23587–23595.

Sanguinetti MC, Jiang C, Curran ME & Keating MT (1995). A mechanistic link between an inherited and an acquired cardiac arrhythmia: HERG encodes the I_{Kr} potassium channel. *Cell* **81**, 299–307.

Snyders DJ & Chaudhary A (1996). High affinity open channel block by dofetilide of HERG expressed in a human cell line. *Mol Pharmacol* **49**, 949–955.

Wang S, Liu S, Morales MJ, Strauss HC & Rasmusson RL (1997*a*). A quantitative analysis of the activation and inactivation kinetics of HERG expressed in *Xenopus* oocytes. *J Physiol* **502**, 45–60.

Wang S, Morales MJ, Liu S, Strauss HC & Rasmusson RL (1997*b*). Modulation of HERG affinity for E-4031 by $[K^+]o$ and C-type inactivation. *FEBS Lett* **417**, 43–47.

Wang S, Morales MJ, Qu YJ, Bett GC, Strauss HC & Rasmusson RL (2003). Kv1.4 channel block by quinidine: evidence for a drug-induced allosteric effect. *J Physiol* **546**, 387–401.

Yeola SW, Rich TC, Uebele VN, Tamkun MM & Snyders DJ (1996). Molecular analysis of a binding site for quinidine in a human cardiac delayed rectifier K^+ channel. Role of S6 in antiarrhythmic drug binding. *Circulation Res* **78**, 1105–1114.

Zagotta WN, Hoshi T & Aldrich RW (1990). Restoration of inactivation in mutants of Shaker potassium channels by a peptide derived from ShB. *Science* **250**, 568–571.

Zhou M, Morais-Cabral JH, Mann S & MacKinnon R (2001). Potassium channel receptor site for the inactivation gate and quaternary amine inhibitors. *Nature* **411**, 657–661.

Acknowledgements

Supported in part by NIH R01 HL-59526-01, NSF KDI grant DBI-9873173, an Established Investigator Award from the American Heart Association, and a grant from the Oishei Foundation.

© The Physiological Society 2003